Combinatorial Biomimetic Chemistry: Parallel Synthesis of a Small Library of β-Hairpin Mimetics Based on Loop III from Human Platelet-Derived Growth Factor B

by **Lujong Jiang**[a]), **Kerstin Moehle**[a]), **Boopathy Dhanapal**[b]), **Daniel Obrecht**[b]), and **John A. Robinson**[a])*

[a]) Institute of Organic Chemistry, University of Zürich, Winterthurerstrasse 190, CH-8057 Zürich
[b]) Polyphor AG, Winterthurerstrasse 190, CH-8057 Zürich

Combinatorial diversity in hypervariable β-hairpin loops is exploited by the immune system to select binding sites on antibodies for a wide variety of different protein antigens. In a first step towards mimicking this strategy *in vitro*, for the selection of novel protein ligands, an approach is described here for the parallel synthesis of small libraries of conformationally defined β-hairpin protein epitope mimetics. Starting from a protruding hairpin loop in platelet-derived growth factor B (PDGF-B), 8 and 12 residues were first transplanted from the protein to a D-Pro-L-Pro template, to afford the cyclic peptide-loop mimetics **1** and **2**, respectively. NMR and MD studies in aqueous solution show that both mimetics populate conformations which closely mimic the β-hairpin in the crystal structure of the native protein (*Fig. 5*). Based on **1** as a scaffold, a library of 24 mimetics was synthesized in which the four residues at the tip of the loop (VRKK) were held constant, and flanking residues at positions 1, 2, 7, and 8 in the hairpin were varied (*Fig. 7*). The library was prepared by parallel synthesis in a two-stage solid-phase assembly/solution-phase cyclization process. The products were analyzed by MS, NMR, and CD. 2D-NOESY revealed for most library members characteristic long-range NOEs that show that the hairpin conformation is stably maintained. The results suggest that this approach may be useful for the synthesis of much larger libraries of peptide and protein mimetics based on a β-hairpin scaffold.

1. Introduction. – Small synthetic molecules that mimic surface epitopes on proteins are a potential source of novel ligands for use in chemical biology, as well as in drug and vaccine design. Already, peptidomimetics of β-turns, β-hairpins, and α-helices have been discovered that imitate the biological activity (*e.g.*, receptor binding, antibody recognition) of an intact native protein (for reviews, see [1][2]). β-Hairpins are frequently involved in protein-protein recognition, and in this context are particularly interesting targets for mimetic design, because two anti-parallel β-strands as well as a β- (or related) turn may be incorporated within one and the same molecule. Moreover, if the β-hairpin mimetic is conformationally well-defined, *i.e.*, the β-hairpin is highly populated in aqueous solution, then the relative positions of backbone and side-chain groups may be accurately mapped in three-dimensional space. This information can be of great value in understanding and developing structure-biological-activity relationships. In this regard, a further significant step can be envisaged in which combinatorial libraries of conformationally defined β-hairpin mimetics are generated by parallel synthesis and screened for biological activity. Of course, a similar principle is used *in vivo* by the immune system during antigen-driven selection, amplification, and maturation of antibodies.

Although substantial progress has been made in the design and synthesis of β-turn mimetics [2][3], still relatively few general methods are available for the production of

β-hairpin epitope mimetics, in particular, where the aim is to provide a good structural mimic of a hairpin in a native protein (for related approaches, see [4–13]). We have exploited here an approach described in earlier work [14–16], where the hairpin structure is transplanted from the protein to a template, whose function is to fix the conformation of the N- and C-terminal loop residues into a β-hairpin geometry. As template, we have used the well-known and readily accessible heterochiral D-Pro-L-Pro unit [17–19], which has been used previously for the design of hairpin mimetics based on antibody hypervariable loops [14], as well as the exposed CC′ loop on the interferon γ receptor [15]. We also chose to develop an efficient parallel-synthesis strategy that affords single compounds in milligram amounts, each amenable to chemical characterization.

To illustrate the approach, we report below the synthesis of a small library of β-hairpin peptidomimetics based on a protruding loop (loop III) in human platelet-derived growth factor B (PDGF-B). The approach, however, is general and may in principle be applied to many other biologically interesting peptides and proteins.

2. Results and Discussion. – 2.1. *Design and Synthesis of Hairpin Mimetics* **1** *and* **2** *of PDGF-BB.* PDGF-BB is a homodimer and a member of the cysteine-knot family of growth factors. Its crystal structure has been reported [20] at 3.2-Å resolution. Each polypeptide chain has two long, twisted antiparallel pairs of β-strands. The strand connections, denoted loops I, II and III, range from residues Ile^{25} to Leu^{38}, Cys^{53} to Val^{58}, and Lys^{74} to Lys^{85}, respectively. In the X-ray crystal stucture of PDGF-BB, most of loop I was structurally undetermined due to a lack of interpretable electron density [20]. The extended and protruding hairpin-loop III lies adjacent to loop I at each end of the homodimer (*Fig. 1*). The loop-III mimetics **1** and **2** were prepared by transferring, respectively, the 8 residues from Glu^{76} to Ile^{83} and the 12 residues from Lys^{74} to Lys^{85}, to a D-Pro-L-Pro template.

Two approaches were investigated for the synthesis of **1** and **2**. In the first approach, a linear peptide precursor was made on *Tentagel S-AC* resin by standard Fmoc chemistry (Fmoc = (9*H*-fluoren-9-ylmethoxy)carbonyl) [21], starting at the C-terminus with Arg. The side-chain-protected linear precursors were then cleaved from the resin with 1% CF_3COOH/CH_2Cl_2, and macrocyclization was performed in DMF. As in earlier work [14][15], the presence of the template near the middle of the linear sequence promoted efficient cyclization. The crude products contained the desired

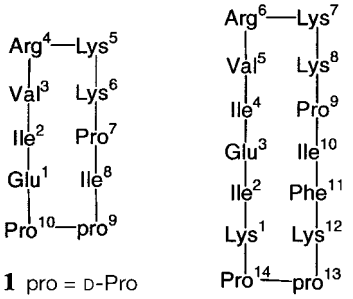

1 pro = D-Pro

2 pro = D-Pro

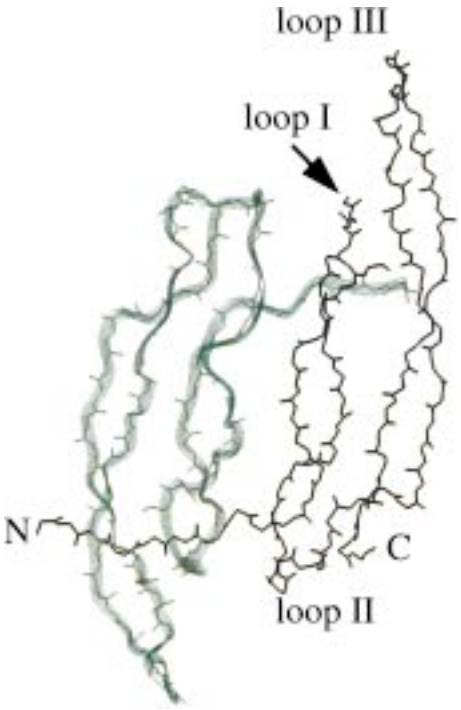

Fig. 1. *PDGF-BB, a line drawing of the backbone of one monomer unit and a ribbon representation of the second subunit* (drawn using the Brookhaven protein databank file 1PDG). The loops I, II, and III of one subunit are indicated. Note that loop I is incomplete in the crystal structure.

cyclic peptides, without significant contamination by oligomeric forms. The yields of **1** and **2** after HPLC purification were *ca.* 68 and 37%, respectively.

In the second approach, the macrocyclization was performed on the resin. Fmoc-Lys-O-allyl (corresponding to Lys^5 and Lys^7 in **1** and **2**) was first coupled to 2-chlorotrityl resin through the side-chain amino group, and the linear precursor was assembled again using standard Fmoc chemistry. The lysine allyl ester was then cleaved with Pd^0, macrocyclization was performed with HATU and HOAt (see *Exper. Part*), and the resin was then treated with CF_3COOH to afford **1** or **2**. HPLC Analysis of the crude product, however, revealed, apart from **1** and **2**, significant quantities of by-products, including dimeric species.

These results show that, in this case of **1** and **2**, cyclization in solution gives a cleaner product and in higher yield than when performed on-resin, also without contamination by significant amounts of oligomeric material. It should be noted, however, that the procedure has so far not been systematically optimized.

2.2. *Conformation of* **1** *and* **2** *in Aqueous Solution*. The structures of **1** and **2** were studied in aqueous solution (pH 5.0, 290 or 300 K) by NMR spectroscopy. 1D ^{1}H-NMR Spectra of both **1** and **2** revealed a single molecular species (> 98%) on the chemical-shift time scale. After assigning the 1D spectra by standard methods [22], ^3J coupling constants, amide-proton H/D exchange rates, amide-proton temperature coefficients,

and NOEs were measured (see *Fig. 2*). The 1D ^{1}H-NMR spectra of **1** and **2** showed no significant changes in shifts or line widths over the concentration range of *ca.* 20–0.1 mM, indicating an absence of aggregation.

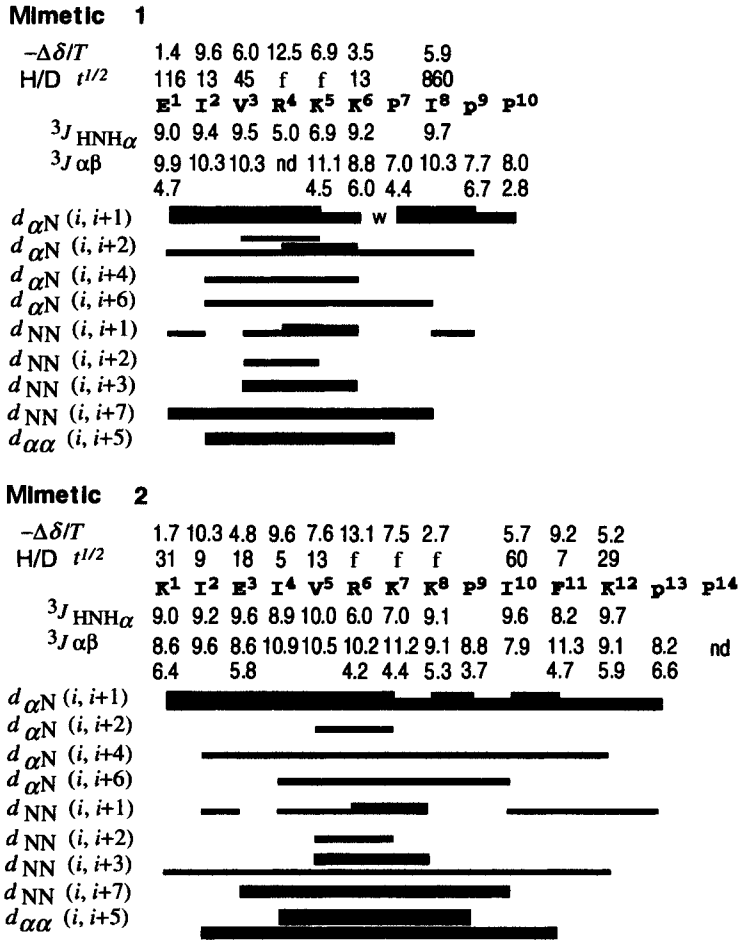

Fig. 2. *NMR Parameters measured for* **1** *and* **2** *in 90% H_2O/D_2O* (pH 5) *at 290 K for* **1** *or at 300 K for* **2**. The amide-proton temperature coefficients $-\Delta\delta$/T [K] were measured over the range 280–320 K. The half-lives $t_{1/2}$ [min] of H/D exchange for amide protons at 290 or 300 K in D_2O (pD* 3.5) were measured by fitting residual peak intensity to an exponential function (f = fast). ^3J Coupling constants [Hz] were from 1D and/or E.COSY plots. The NOE connectivities (fat line = strong NOE, thin line = weak NOE) were measured from NOESY plots. w = NOE obscured by H_2O resonance; p = D-Pro.

The NMR data provide evidence that both mimetics adopt a stable β-hairpin geometry, the most conclusive being the appearance of characteristic long-range NOEs in 2D NOESY plots. Numerous NOEs are observed between groups far apart in the sequence, but close in space across the β-hairpin. These include NOEs between the H–C(α) protons of Ile^2 and Pro^7 in **1**, and of Ile^2 and Phe^{11} and of Ile^4 and Pro^9 in **2** (Fig. 3). Similarly, strong d_{NN} NOEs are seen between Val^3 and Lys^6, as well as Glu^1 and

Ile[8] in **1**, and Val[5] and Lys[8], Glu[3] and Ile[10], as well as Lys[1] and Lys[12] in **2**. The presence of β-hairpin conformations is also consistent with the >9.0 Hz $^3J(\mathrm{HN,H}\alpha)$ values observed for both mimetics (*Fig. 2*). Average solution structures were calculated for **1** and **2** using distance restraints derived from NOE build-up curves, by restrained dynamic simulated annealing (SA), as described elsewhere [23][24].

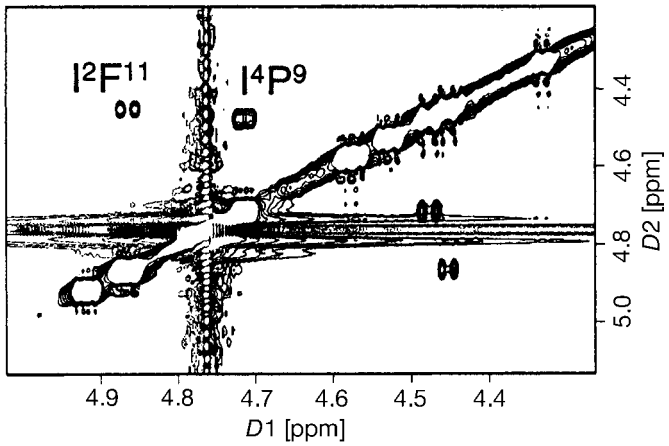

Fig. 3. *The H–C(α)/H–C(α) region of a 2D NOESY plot of* **2** *in* D_2O (pH 5.0) *at 300 K*. The NOE cross-peaks for the NOEs between Ile[2] H–C(α) and Phe[11] H–C(α), as well as between Ile[4] H–C(α) and Pro[9] H–C(α) are indicated. The distortion in both dimensions is due to residual H_2O without presaturation.

From the SA calculations for **1**, the resulting low-energy structures could be superimposed over the backbone N, C(α), and C atoms with a pairwise r.m.s. deviation of only 0.29 ± 0.11 Å (*Fig. 4*). The 22 structures used were within 20 kcal/mol of the lowest-energy structure. Whereas eight showed no distance-restraint violations >0.5 Å, several others showed violations in the range 0.5–0.6 Å for the $d_{\alpha\mathrm{N}}(i, i+1)$ Val[3]-Arg[4] as well as Arg[4]-Lys[5] connectivities. These violations appear to reflect mobility in the Val[3]-Arg[4] and Arg[4]-Lys[5] amide planes. As is apparent from the lowest-energy structure shown in *Fig. 5,a*, the backbone of **1** adopts a well-defined β-hairpin geometry, with cross-strand backbone-backbone H-bonds involving the amide NHs of Glu[1], Val[3], Lys[6], and Ile[8]. These NHs also exchange more slowly with D in the solvent than the other amide NHs (see *Fig. 2*). Importantly, these four NH groups participate in long-range NOE connectivities to groups on the other side of the hairpin (*vide supra*), which constitute a signature of the β-hairpin structure. This point becomes useful later in the analysis of related structures in the combinatorial library (*vide infra*).

In the case of mimetic **2**, low-energy structures were derived by SA that could be superimposed over the backbone N, C(α), and C atoms with a pairwise r.m.s. deviation of 1.0 ± 0.5 Å (*Fig. 4*). The lowest-energy structure is typical of the group (*Fig. 5,b*), and displays a regular β-hairpin geometry with cross-strand backbone-backbone H-bonds involving the amide NHs of Lys[1], Glu[3], Val[5], Lys[7], Ile[10], and Lys[12]. This is consistent with the observation that the amide NHs with relatively slow H/D exchange rates are those of Lys[1], Ile[10], and Lys[12]. The amide NHs at the tip of the hairpin exchange more rapidly under the conditions studied (*Fig. 3*).

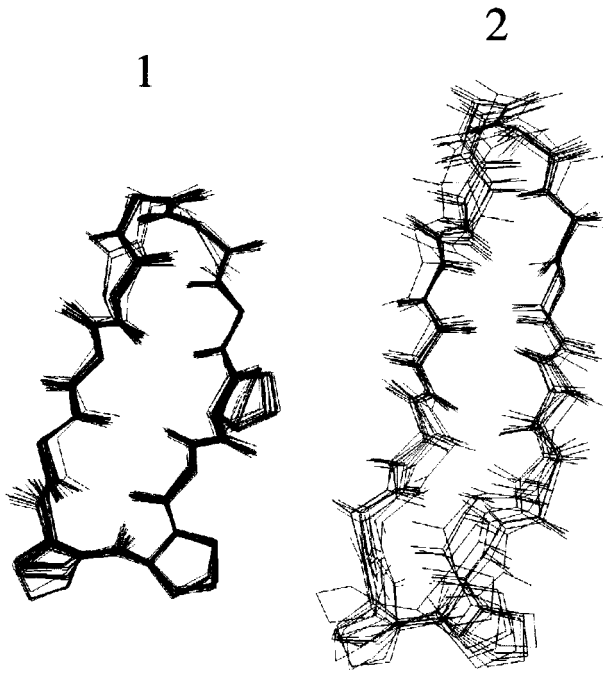

Fig. 4. *Superimpositions over the backbone C, N, and C(α) atoms of the average solution structures determined for* **1** *and* **2** *by dynamic simulated annealing* (see *Sect. 2*)

The energy-minimum structures of **1** and **2** deduced by SA were also used as a starting point for molecular-dynamics (MD) simulations at 300 K in explicit H_2O solvent using the GROMOS96 programs, both with and without time-averaged distance restraints (TA-DR) [25]. Good agreement between the simulated and experimental properties are found in the simulations with **1** and **2**. In the simulation of **1** with TA-DR, the 68 distance restraints are well-satisfied with a small sum of violations (6.62 Å) and the largest single violation being < 1.0 Å. The average coupling constants show violations for several backbone $^3J(\mathrm{HN,H}\alpha)$ values in the range 0.3 – 1.8 Hz. Only the distance violations become larger in the unrestrained simulation, with a sum of violations of 29.7 Å and the largest being 3.83 Å. The fluctuations in backbone ϕ and ψ angles along the hairpin are rather small in both simulations (*Table 1*), with only the tip region (Val^3 to Lys^6) showing small differences between the restrained and unrestrained simulations. During the simulation with TA-DR, mainly a βI′/βIII′ turn is populated, whereas during the unrestrained simulation, a βII turn-like structure (with a γ-turn involving Lys^4) is also significantly populated. In both simulations, three well populated cross-strand backbone-backbone H-bonds are found (*Fig. 6*). The population of all three simultaneously would correspond to a class 2 : 2 β-hairpin, the most abundant β-hairpin type found in high-resolution protein crystal structures [26][27]. The most frequently found turn types in 2 : 2 β-hairpins in proteins are the type I′ and II′, consistent with the predominant βI′/βIII′ turn in the simulation with TA-DR. There is a good qualitative correlation between the involvement of amide NHs in intra-

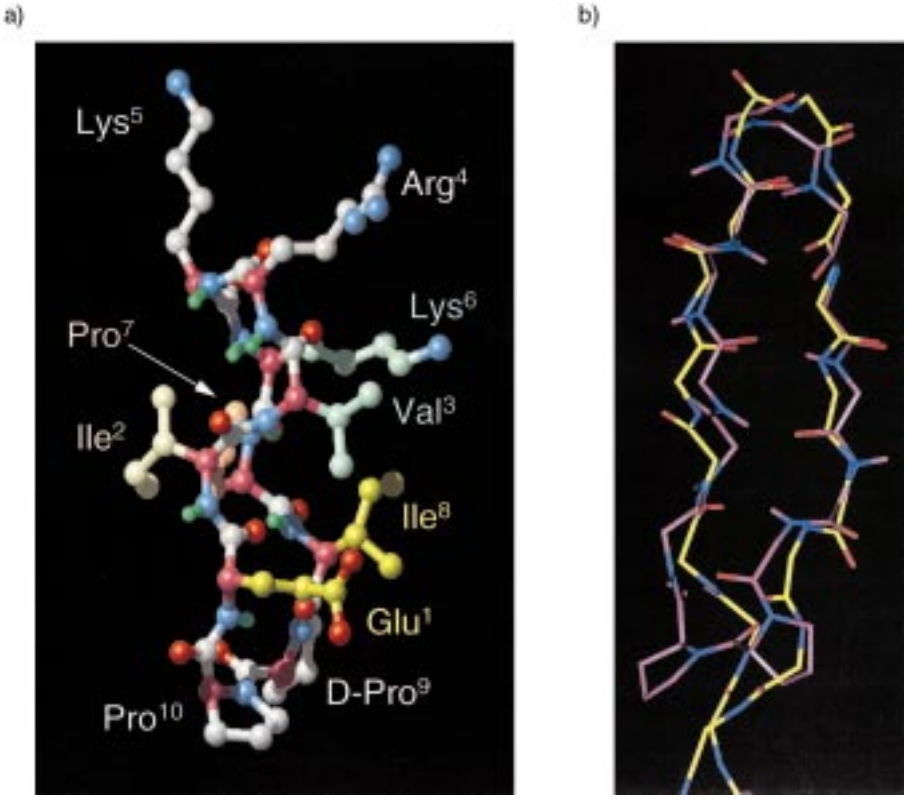

Fig. 5. a) *Solution structure of* **1**, with the D-*Pro*-L-*Pro template at the bottom* (O-atoms = red, N-atoms = blue, C(α) = violet). b) *Comparison of the solution structure of the mimetic* **2** *and loop III in the crystal structure of PDGF-BB* (yellow = PDGF-BB crystal structure, purple = mimetic, O-atoms = red, N-atoms = blue).

molecular H-bonding, indicated experimentally by relatively slow H/D exchange rates (*Fig. 2*), and the population of H-bonds during the simulations (*Fig. 6*).

Over the course of both restrained and unrestrained simulations of mimetic **2**, only small fluctuations of backbone ϕ and ψ angles are observed (*Table 1*), indicating a stable β-hairpin structure. The tip of the hairpin (Val^5 to Lys^8) adopts a stable βI′/βIII′-turn conformation. The sum of distance violations are small in both simulations, with maximum violations < 1.0 Å, indicating a good agreement with the experimental NOE data. The backbone peptide NH groups of Lys^1, Glu^3, Val^5, Lys^8, Ile^{10}, and Lys^{12} participate in cross-strand H-bonding, as typically found in β-hairpin structures (*Fig. 6*). This behavior in the simulations is again in good agreement with the experimental rates of H/D exchange for these protons (*Fig. 2*), although residues closest to the template have a significantly slower exchange rate compared to those nearer to the tip of the hairpin. Throughout both simulations, all the distances between the C(β) atoms of adjacent residues across the hairpin (*i.e.*, C(β)(Val^5)-C(β)(Lys^8), C(β)(Ile^4)-C(β)(Pro^9), C(β)(Glu^3)-C(β)(Ile^{10}), C(β)(Ile^2)-C(β)(Phe^{11}), C(β)(Lys^1)-C(β)(Lys^{12})) remain in the range $5-6 \pm 1$ Å.

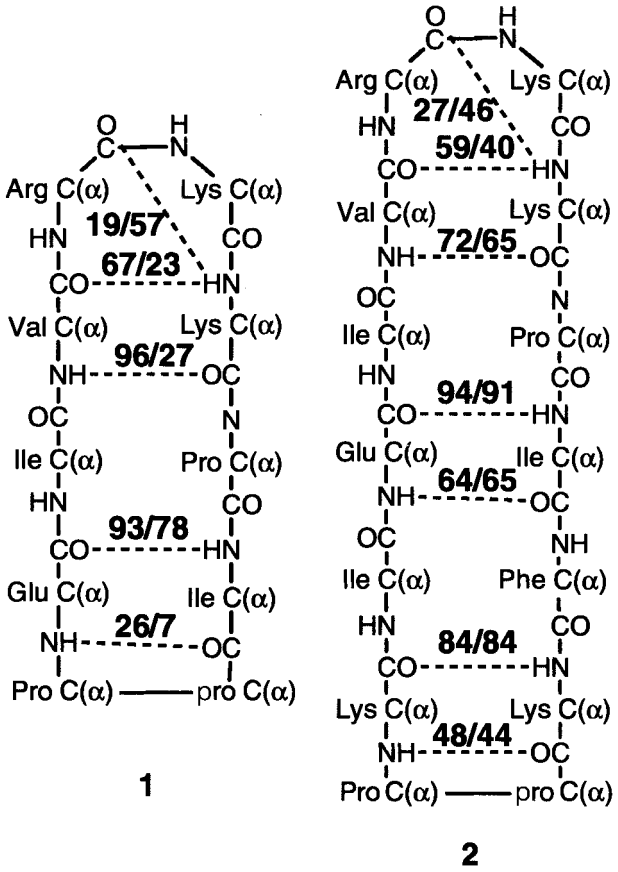

Fig. 6. *H-Bonds established by MD simulations.* The numbers in bold indicate the percentage population of H-bonds during the 2-ns MD simulations both with and without TA-DR (with/without); H-bonds are identified using the criteria H–A distance <2.5 Å and D–H–A angle $>135°$. pro = D-Pro.

In summary, the simulations indicate only limited motional averaging within the backbones of both mimetics on the nanosecond timescale, and reinforce the conclusion that both molecules adopt a well-defined β-hairpin conformation in aqueous solution.

2.3. *Comparison of the Mimetics with PDGF-BB.* The backbone N, C(α), and C atoms of residues Lys^1 to Lys^{12} in the mimetic **2** and the corresponding atoms in the hairpin loop in the crystal structure of PDGF-BB can be superimposed with an r.m.s. deviation of only 0.87 Å, showing that the average solution structure is a very close mimetic of the hairpin in the protein (*Fig. 5,b*). For residues Glu^1 to Ile^8 in mimetic **1**, the r.m.s. deviation is only 0.62 Å. The only significant difference between the NMR and crystal structures in terms of backbone ϕ/ψ angles involves the Arg^6/Lys^7 amide plane in the β-turn at the tip of the loop. A type-II′ β-turn is seen in the protein crystal structure, but a type-I′/III′ β-turn is observed in the NMR structures of **1** and **2**. The crystal structure, however, is of low resolution (3.2 Å), so the orientation of this amide plane in the protein is probably poorly defined.

Table 1. *Backbone Torsion Angles for Each Residue in* **1** and **2** [a])

Residue [b])		Crystal	MD with TA-DR	
			mimetic **1**	mimetic **2**
Lys^{1}	ϕ	− 90.1		− 99.6 ± 27.4
	ψ	83.4		137.9 ± 20.3
Ile^{2}	ϕ	− 72.3		− 101.0 ± 18.5
	ψ	104.7		98.9 ± 19.4
Glu^{3}(1)	ϕ	− 104.8	− 64.8 ± 17.7	− 91.6 ± 20.9
	ψ	123.6	136.7 ± 15.0	129.2 ± 18.5
Ile^{4}(2)	ϕ	− 89.2	− 95.4 ± 15.4	− 92.0 ± 16.4
	ψ	121.6	102.9 ± 12.0	92.9 ± 29.9
Val^{5}(3)	ϕ	− 122.5	− 117.6 ± 12.6	− 107.2 ± 19.7
	ψ	116.2	107.5 ± 13.0	109.6 ± 17.5
Arg^{6}(4)	ϕ	73.9	51.6 ± 10.4	49.2 ± 22.1
	ψ	− 73.0	54.0 ± 12.4	67.6 ± 16.7
Lys^{7}(5)	ϕ	− 146.1	65.4 ± 10.5	64.2 ± 10.7
	ψ	8.4	− 1.9 ± 24.7	-8.8 ± 26.8
Lys^{8}(6)	ϕ	− 144.1	− 102.4 ± 23.7	− 104.8 ± 21.8
	ψ	142.9	127.7 ± 12.1	114.7 ± 13.5
Pro^{9}(7)	ϕ	− 92.0	− 68.1 ± 9.3	− 73.5 ± 10.6
	ψ	132.0	109.0 ± 12.8	112.4 ± 18.5
Ile^{10}(8)	ϕ	− 101.9	− 104.7 ± 13.0	− 112.9 ± 18.7
	ψ	149.8	90.5 ± 9.0	132.7 ± 17.2
Phe^{11}	ϕ	− 114.4		− 75.7 ± 17.3
	ψ	57.7		108.5 ± 13.9
Lys^{12}	ϕ	− 48.5		− 118.3 ± 12.7
	ψ	126.7		89.0 ± 11.0
Pro^{13}(9)	ϕ		61.2 ± 8.2	58.3 ± 9.0
	ψ		− 126.8 ± 13.1	− 121.1 ± 14.2
Pro^{14}(10)	ϕ		− 72.1 ± 12.4	− 66.9 ± 12.4
	ψ		− 40.8 ± 16.2	− 33.3 ± 22.5

[a]) The averages and r.m.s. deviations over the course of the 2-ns molecular-dynamics (MD) simulations with TA-DR in comparison to the corresponding angles from the crystal structure of PDGF-BB (Crystal). [b]) The sequence numbers for mimetic **1** are in parentheses.

2.4. *Library Design and Synthesis.* Based on the stable β-hairpin in **1** as a scaffold, the small 24-member library shown in *Fig. 7* was designed. The four residues Val-Arg-Lys-Lys (VRKK) at the tip of the loop were held constant, and the residues at positions 1, 2, 7, and 8 were varied, in particular, to include the aromatic amino acids Tyr(Y) and Trp(W), amongst others. The design was guided partly by mutagenesis data showing that the basic RKK sequence in loop I may be important for receptor binding [28–30], and the observation that Tyr and Trp residues are frequently located in hot-spots at protein-protein interfaces [31].

The parallel synthesis of all 24 mimetics was performed using a manual 24-reactor workstation. The construction of the linear precursors was initiated with residue Arg^{4} at the C-terminus, and was elaborated using Fmoc solid-phase peptide chemistry [21] on 2-chlorotrityl resin. When the assembly of the 10-residue linear precursors was complete, the N-terminal Fmoc group was removed, and the side-chain-protected linear peptides were cleaved from the resin with 1% CF_3COOH in CH_2Cl_2. The purity of each linear precursor was assayed at this stage by reversed-phase HPLC. Again in

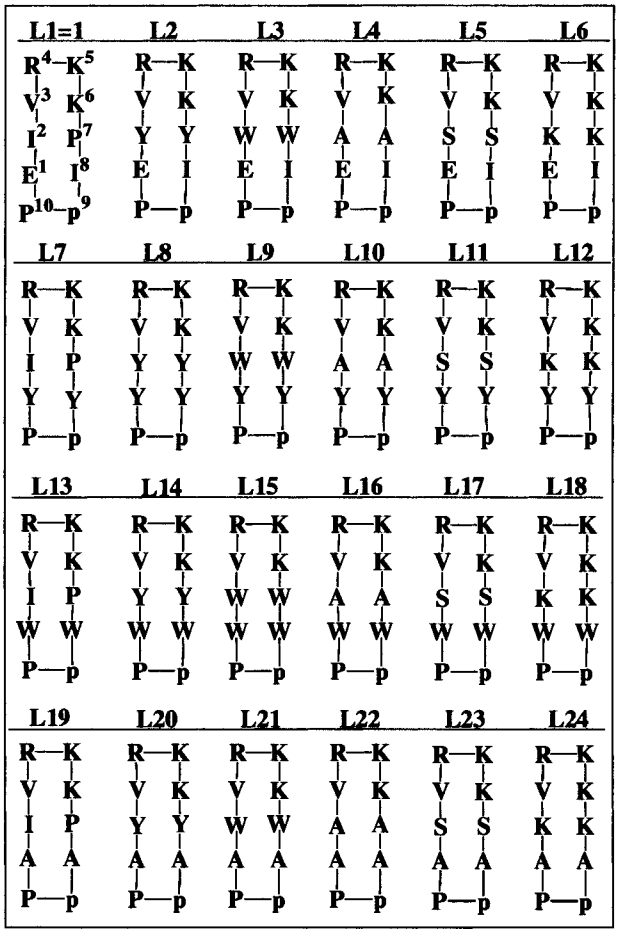

Fig. 7. *Sequences of the 24-member library of hairpin mimetics.* The loop **L1** corresponds to the mimetic **1** with the wild-type sequence. p = D-Pro.

parallel, the linear precursors were cyclized in dilute DMF solution using HOAt and HATU for activation (see *Exper. Part*). Finally, the cyclic products were directly treated with CF_3COOH containing 2.5% of H_2O and 2.5% of triisopropylsilane as scavengers for 2 h at room temperature. After drying *in vacuo*, all the products **L1**–**L24** were characterized.

2.5. *Characterization of the Library.* The purity of the final crude cyclic products **L1**–**L24** was assayed by reversed-phase HPLC. The chromatograms showed in each case a major peak corresponding to the desired mimetic. In 16 out of 24 cases, this major peak was 80–90% of the total product recorded on the chromatogram. In 7 cases (**L3**, **L9**, **L12**, **L16**, **L18**, **L20**, and **L21**), the major peak was 60–80% of the total, and for one mimetic (**L15**), the major peak was only *ca.* 30–40% of the total. The library synthesis was repeated, with largely similar results. In general, the linear protected

peptides were transformed into cyclic protected peptides with comparable purity. By-products arose, however, during side-chain deprotection in mimetics having a high content of Trp(W) residues. However, by reducing the time for deprotection in CF_3COOH from 2 h to 30 min, the purities of the mimetics **L3** and **L9** (both now $>80\%$) and **L15** (now ca. 70%) could be significantly improved.

To establish that the major peaks identified by HPLC in the crude products are the desired mimetics, all 24 were purified by HPLC and characterized by electrospray (ES) MS, NMR (1D ^{1}H-NMR, 2D TOCSY, DQF-COSY, and NOESY and/or ROESY), and CD spectroscopy. All purified samples gave a strong molecular ion by ES-MS consistent with the expected masses (see *Exper. Part*). The ^{1}H-NMR spectra measured in H_2O/D_2O (9:1 except for **L15** in CD_3OD/H_2O 1:1) were particularly informative, since the low-field region between 6–10 ppm gives a clear indication of the number of peptide amide protons, and hence of the purity and conformational heterogeneity of the mimetic. With some interesting exceptions, all the samples showed 7 or 8 amide protons, and the spectra were consistent with each major product in the HPLC being a single molecular species ($>95\%$) on the chemical-shift time-scale, with the expected constitution.

The mimetics **L20**–**L24**, however, each revealed 16 amide-proton resonances, suggesting the presence of *trans/cis* peptide bond rotamers in a *ca.* 4:1 to 2:1 ratio. A chirality analysis of the mimetics, by means of a modified *Marfey*'s reagent N^2-(5-fluoro-2,4-dinitrophenyl)-L-valinamide [32] and the peptide hydrolysate, showed as expected only one D-amino acid (D-proline). On the other hand, no chemical-exchange peaks in the amide region were seen in the 2D ROESY plots measured at 300 K. That the minor set of amide resonances originates from a *cis* rotamer at the Ala^8-D-Pro^9 peptide bond was clearly shown, however, by the observation of a strong $d_{\alpha\alpha}(i, i+1)$ NOE between Ala^8 and D-Pro^9 in NOESY and/or ROESY spectra. It is notable that the *cis* rotamer is only observed in the mimetics **L20**–**L24**.

It is reasonable to expect that the conformation of the mimetics might be influenced as the sequence of the loop is varied. To address this question, the preferred loop conformations of **L2**–**L24** were studied by NMR and CD. CD Spectra were measured in H_2O (pH 5.0) (except for **L15** in MeOH/H_2O 1:1). The CD spectrum of **L1** (*Fig. 8*) showed a single negative peak at 222 nm, a very low molar ellipticity above 250 nm, and a transition to positive ellipticity below 200 nm. This spectrum appears to be typical of a β-hairpin peptide lacking aromatic groups [33]. The CD spectra of **L3**, **L9**, **L15**, and **L21**, however, now showed an exciton couplet at 222 nm, with a negative peak at 215 nm and a positive peak at 223 nm (*e.g.*, for **L3**, see *Fig. 8*). A similar spectrum was observed earlier for an antibody CDR mimetic [14], also having Trp residues at positions 2 and 7 in an 8-residue hairpin mimetic. The exciton couplet is consistent with the interaction of the indole rings, due to their proximity to each other on one side of the hairpin. The peaks assigned to the exciton couplet were much weaker, however, in the CD spectra of mimetics **L13**, **L14** and **L16**–**L18** that have Trp residues at positions 1 and 8 in the hairpin. The mimetics **L2**, **L8**, **L14**, and **L20** all gave similarly shaped CD curves having a more complex pattern of overlapping peaks (data not shown). The remaining mimetics gave CD spectra largely similar in shape to those found for the **L1** loop mimetic.

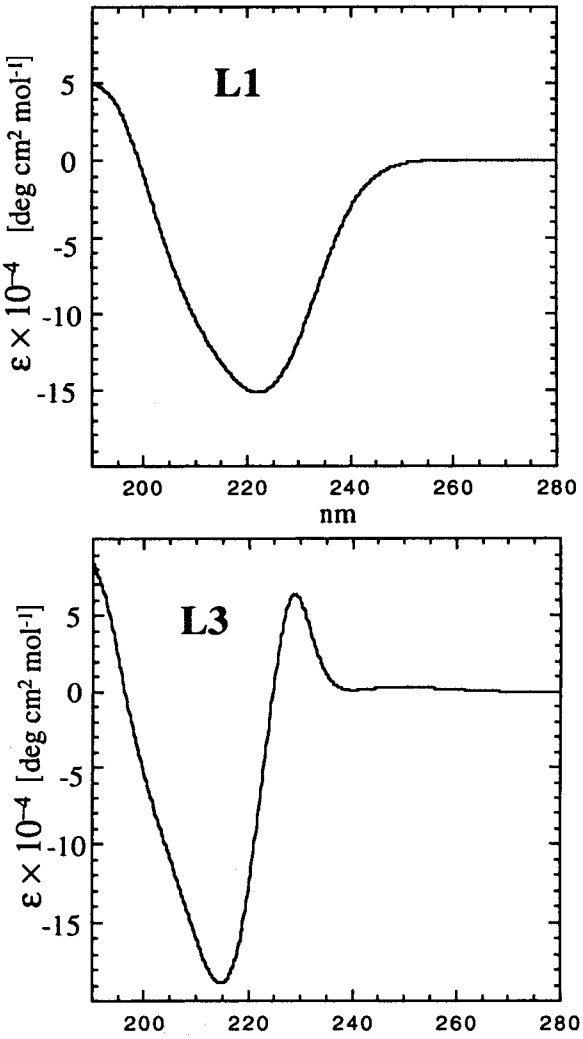

Fig. 8. *CD Spectra of mimetics* **L1** *and* **L3** *in water* (pH 5)

More conclusive evidence for the maintenance of a β-hairpin conformation was found in NOESY plots recorded in H_2O/D_2O 9 : 1 (except for **L15** in CD_3OD/H_2O 1 : 1). Most of the mimetics gave NOESY and/or ROESY plots showing characteristic long-range d_{NN} NOEs between the amide NH protons in residues 1 and 8, as well as between residues 3 and 6, as seen also in the wild-type loop **L1** (*Fig. 2*). Although variations in the extents of motional averaging from one mimetic to the next cannot be ruled out, the appearance of these long-range d_{NN} NOEs shows that the β-hairpin conformation remains significantly populated. The exceptions were **L22**–**L24**, where now all $d_{NN}(i,\ i+1)$ NOEs, and the long-range signature NOEs were weak or absent. Therefore, the hairpin conformation in these mimetics appears to have been disrupted,

and this occurs concomitantly with the population of a *cis* Ala[8]-D-Pro[9] peptide bond (*vide supra*). While the precise reasons for these differences remain to be determined, it appears that the hairpin stability can be adversely affected by the loop sequence, and in particular by Ala residues adjacent to the template, in at least some of these mimetics. Notwithstanding this, for most of the library, the NMR and CD data provide strong evidence that the β-hairpin conformation has been retained in aqueous solution.

In conclusion, a method has been established to create combinatorial diversity around a conformationally well-defined peptide mimetic scaffold, the β-hairpin. Although one swallow does not make a summer, these results provide motivation to develop the technology for the production of much larger libraries of β-hairpin mimetics. These libraries may prove to be a useful source of novel ligands for drug and vaccine research. The PDGF antagonist activity of the library of β-hairpin-loop mimetics described here will be reported in future work.

This work was supported by grants from the *Swiss National Science Foundation.* The authors thank Prof. *Wilfred van Gunsteren* (ETH-Zürich) for the GROMOS96 suit of programs, and *Martin Binder*, *Nadja Walch*, and Dr. *Gudrun Hopp-Rentsch* for valuable assistance with NMR spectra.

Experimental Part

Abbreviations. CIP, 2-chloro-1,3-dimethylimidazolidinium hexafluorophosphate; DMF, N,N-dimethylformamide; HATU, 2-(1*H*-7-azabenzotriazol-1-yl)-1,1,3,3-tetramethyluronium hexafluorophosphate (=2-(1*H*-1,2,3-triazolo[4,5-*b*]pyridin-1-yl)-1,1,3,3-tetramethyluronium hexafluorophosphate); HBTU, 2-(1*H*-benzotriazol-1-yl)-1,1,3,3-tetramethyluronium hexafluorophosphate; HOAt, 1-hydroxy-7-aza-1*H*-benzotriazole (=1-hydroxy-1*H*-1,2,3-triazolo[4,5-*b*]pyridine); HOBt, 1-hydroxy-1*H*-benzotriazole; Pmc, (2,2,5,7,8-pentamethylchroman-6-yl)sulfonyl.

Cyclo(-Glu-Ile-Val-Arg-Lys-Lys-Pro-Ile-d-Pro-Pro-) (**1**) and Cyclo(-Lys-Ile-Glu-Ile-Val-Arg-Lys-Lys-Pro-Ile-Phe-Lys-d-Pro-Pro-) (**2**). For **1**, the first amino acid Fmoc-Arg(Pmc)-OH (249 mg, 3 equiv.) was coupled to *Tentagel S-AC* resin (0.4 g, 0.29 mmol/g) in the presence of CIP (195 mg, 6 equiv.) in CH_2Cl_2/pyridine 1:1 (2 ml), with swirling for 2 h. Then by standard Fmoc chemistry [21], a linear peptide was constructed: H-Lys(Boc)-Lys(Boc)-Pro-Ile-d-Pro-Pro-Glu(OtBu)-Ile-Val-Arg(Pmc)-O-resin. The linear peptide was cleaved from the resin with 1% CF_3COOH in CH_2Cl_2 and the soln. neutralized with pyridine, washed with H_2O, and evaporated to give a crude linear product H-Lys(Boc)-Lys(Boc)-Pro-Ile-D-Pro-Pro-Glu(O^{t}Bu)-Ile-Val-Arg(Pmc)-OH (150 mg). Cyclization was performed in DMF (150 ml, *ca.* 1 mg/ml) with HATU (101 mg, 3 equiv.), HOAt (36 mg, 3 equiv.), and ^{i}Pr$_2$EtN (1.5 ml; 1% v/v), with stirring overnight. The cyclization was monitored by reversed-phase HPLC (*C18* column, 5–100% MeCN/H_2O + 0.1% CF_3COOH over 25 min). Upon completion, DMF was evaporated in vacuo, the residue dissolved in CH_2Cl_2, and the soln. extracted with 10% MeCN/H_2O and evaporated to give the cyclized peptide with side-chain protecting groups. This was deprotected with CF_3COOH/^{i}Pr$_3$SiH/H_2O 95:2.5:2.5, and 1 was purified by reversed-phase HPLC (*C18* column, 10–60% MeCN/H_2O + 0.1% CF_3COOH over 20 min): 73 mg (68%) of **1**. By the same procedure, **2** (37%) was obtained. ES-MS: **1**: 580.02 ([M + 2 H]$^{2+}$); **2**: 838.7 ([M + 2 H]$^{2+}$). ^{1}H-NMR (600 MHz, D_2O/H_2O 1:9, pH 5.0), see *Tables 2* and *3*.

Synthesis of **1** *by Cyclization On-Resin*. Fmoc-Lys-O-allyl (1 equiv.) was linked to 2-chlorotrityl chloride resin (1.25 mmol/g) with ^{i}Pr$_2$EtN (3 equiv.) in CH_2Cl_2, with swirling overnight at r.t. The linear peptide was assembled using standard Fmoc chemistry, with protected amino acids (4 equiv.), HBTU (4 equiv.), HOBt (4 equiv.), and ^{i}Pr$_2$EtN (6 equiv.) in DMF and a coupling time of 1.5–2 h. The allyl ester group was removed by treatment with [Pd(PPh$_3$)$_4$] (0.2 equiv.), trimethylsilyl azide (8 equiv.) and $Bu_4NF \cdot 3\ H_2O$ (3 equiv.) in CH_2Cl_2 for 30 min. The resin was filtered and washed successively with CH_2Cl_2, 0.5% (*v*/*v*) ^{i}Pr$_3$SiH in DMF, 0.5% sodium diethylcarbamodithioate in DMF, MeOH, and finally CH_2Cl_2. Deprotection was monitored by reversed-phase HPLC (*C18* column, 50–100% MeCN/H_2O + 0.1% CF_3COOH over 20 min). After removal of the Fmoc group with 20% piperidine in DMF, the cyclization was performed with HATU (3 equiv.), HOAt (3 equiv.), and ^{i}Pr$_2$EtN (4.5 equiv.) in DMF for 2 h. Upon completion, the peptide was cleaved from the resin with CF_3COOH/

Table 2. *^{1}H-NMR* (600 MHz) *Chemical Shifts* [a]) [ppm] *for* **1** *at 290 K in 10% D_2O/H_2O* (pH 5.0)

Residue	NH	H–C(α)	H–C(β) [b])	Others [b])
Glu[1]	7.71	4.62	1.94, 2.03	$CH_2(\gamma)$ 2.28, 2.23
Ile[2]	8.57	4.46	1.79	$CH_2(\gamma)$ 1.03, 1.42; $CH_3(\gamma)$ 0.64; $CH_3(\delta)$ 0.72
Val[3]	8.80	4.21	1.97	$CH_3(\gamma)$ 0.89, 0.92
Arg[4]	9.46	3.88	1.88	$CH_2(\gamma)$ 1.62; $CH_2(\delta)$ 3.21, 3.29; NH(ε) 7.29
Lys[5]	8.37	3.58	1.99, 2.18	$CH_2(\gamma)$ 1.34; $CH_2(\delta)$ 1.67; $CH_2(\varepsilon)$ 2.98
Lys[6]	7.96	4.91	1.78, 1.92	$CH_2(\gamma)$ 1.41, 1.50; $CH_2(\delta)$ 1.72; $CH_2(\varepsilon)$ 3.03
Pro[7]	–	4.78	1.98, 2.23	$CH_2(\gamma)$ 1.99, 2.24; $CH_2(\delta)$ 3.74, 3.89
Ile[8]	8.77	4.53	1.87	$CH_2(\gamma)$ 1.13, 1.52; $CH_3(\gamma)$ 0.87; $CH_3(\delta)$ 0.84
D-Pro[9]	–	4.77	1.90, 2.33	$CH_2(\gamma)$ 2.03, 2.16; $CH_2(\delta)$ 3.50, 3.87
Pro[10]	–	4.57	2.22	$CH_2(\gamma)$ 1.97, 2.10; $CH_2(\delta)$ 3.73, 4.01

[a]) Chemical shifts are measured relative to internal TSP (sodium (trimethylsilyl)(D_4)propanoate). [b]) Diastereotopic H-atoms are not assigned.

Table 3. *^{1}H-NMR* (600 MHz) *Chemical Shifts* [a]) [ppm] *for* **2** *at 300 K in 10% D_2O/H_2O* (pH 5.0)

Residue	NH	H–C(α)	H–C(β) [b])	Others [b])
Lys1	7.69	4.53	1.85, 1.90	$CH_2(\gamma)$ 1.42; $CH_2(\delta)$ 1.71; $CH_2(\varepsilon)$ 3.01
Ile[2]	8.24	4.45	1.50	$CH_2(\gamma)$ 0.55, 1.30; $CH_3(\gamma)$ 0.56; $CH_3(\delta)$ 0.68
Glu[3]	8.79	4.58	1.72, 1.89	$CH_2(\gamma)$ 2.12
Ile[4]	8.55	4.47	1.83	$CH_2(\gamma)$ 1.10, 1.36; $CH_3(\gamma)$ 0.60; $CH_3(\delta)$ 0.61
Val[5]	8.77	4.18	1.91	$CH_3(\gamma)$ 0.85; 0.91
Arg[6]	9.45	3.84	1.88, 1.90	$CH_2(\gamma)$ 1.62; $CH_2(\delta)$ 3.20, 3.27; NH(ε) 7.23
Lys[7]	8.31	3.52	2.00, 2.18	$CH_2(\gamma)$ 1.33; $CH_2(\delta)$ 1.67; $CH_2(\varepsilon)$ 2.98
Lys[8]	7.89	4.91	1.77, 1.89	$CH_2(\gamma)$ 1.41, 1.51; $CH_2(\delta)$ 1.72; $CH_2(\varepsilon)$ 3.04
Pro[9]	–	4.71	1.57, 1.83	$CH_2(\gamma)$ 1.96, 2.18; $CH_2(\delta)$ 3.73, 3.80
Ile[10]	9.08	4.33	1.89	$CH_2(\gamma)$ 1.22, 1.40; $CH_3(\gamma)$ 0.87; $CH_3(\delta)$ 0.80
Phe[11]	8.51	4.86	2.93, 3.21	Ph–H 7.28
Lys[12]	8.92	4.87	1.66, 1.76	$CH_2(\gamma)$ 1.30, 1.34; $CH_2(\delta)$ 1.62; $CH_2(\varepsilon)$ 2.86, 2.92
D-Pro[13]	–	4.87	1.92, 2.30	$CH_2(\gamma)$ 2.00, 2.16; $CH_2(\delta)$ 3.49, 3.83
Pro[14]	–	4.58	2.27	$CH_2(\gamma)$ 1.94, 2.12; $CH_2(\delta)$ 3.75, 4.02

[a]) Chemical shifts are measured relative to internal TSP (sodium (trimethylsilyl)(D_4)propanoate). [b]) Diastereotopic H-atoms are not assigned.

^{i}Pr$_3$SiH/H_2O 95:2.5:2.5 and purified by reversed-phase HPLC (*C18* column, 5–50% MeCN/H_2O + 0.1% CF_3COOH over 20 min): **1** (36%).

Parallel Synthesis of Cyclo(-X^1-X^2-Val-Arg-Lys-Lys-X^7-X^8-D-Pro-Pro-) (**L1**–**L24**; see *Fig. 7*). Fmoc-Arg(Pmc)-OH (1 equiv.) was linked to 2-chlorotrityl chloride resin (960 mg, 1.25 mmol/g) with ^{i}Pr$_2$EtN (3 equiv.) in CH_2Cl_2, with swirling overnight at r.t. The resin was then divided into 24 equal parts and placed in 24 separate reaction vessels. The linear peptides were assembled by standard Fmoc chemistry, with protected amino acids (4 equiv.), HBTU (4 equiv.), HOBt (4 equiv.), and ^{i}Pr$_2$EtN (6 equiv.) in DMF and a coupling time of 1.5–2 h. The 24 linear peptides with side-chain protecting groups were cleaved from the resin with 1% CF_3COOH in CH_2Cl_2 (2 × 10 min) and the solns. neutralized with pyridine (1 equiv.) in 24 flasks and then evaporated.

The linear precusors obtained (without purification) were directly cyclized at a concentration of 1 mg/ml in DMF using HATU (3 equiv.), HOAt (3 equiv.), and ^{i}Pr$_2$EtN (1% *v/v*), with swirling for 16 h. The DMF was then evaporated from each flask, 10% MeCN/H_2O was added to each residue, and then CH_2Cl_2 to dissolve the precipitate. The upper aq. phase was carefully removed, and the CH_2Cl_2 phase was washed with H_2O, and then evaporated. To each residue, CF_3COOH/^{i}Pr$_3$SiH/H_2O 95:2.5:2.5 was added and the mixture left at r.t. for 2 h. The soln. was then evaporated, the peptide precipitated with cold Et_2O, and the Et_2O removed after centrifugation. Each crude peptide was analyzed and purified by HPLC (*C18* column, 20–65% MeCN/H_2O +

Table 4. *ES-MS (m/z) of β-Hairpin Mimetics* **L1** – **L24**

Peptide	Formula	M_r	ES-MS		
			$[M+H]^+$	$[M+2H]^{2+}$	$[M+3H]^{3+}$
L1	$C_{55}H_{95}N_{15}O_{12}$	1158.5	–	580.02	387.02
L2	$C_{62}H_{95}N_{15}O_{14}$	1274.5	1274.8	638.01	425.75
L3	$C_{66}H_{97}N_{17}O_{12}$	1320.6	1320.81	661.06	441.11
L4	$C_{50}H_{87}N_{15}O_{12}$	1090.3	1090.54	545.83	364.26
L5	$C_{50}H_{87}N_{15}O_{14}$	1122.3	1122.71	562.07	375.05
L6	$C_{56}H_{101}N_{17}O_{12}$	1204.5	1205.7	603.18	402.58
L7	$C_{62}H_{95}N_{15}O_{12}$	1242.5	–	621.90	414.89
L8	$C_{69}H_{95}N_{15}O_{14}$	1358.6	–	679.82	453.61
L9	$C_{73}H_{97}N_{17}O_{12}$	1404.7	1404.83	703.08	469.16
L10	$C_{57}H_{87}N_{15}O_{12}$	1174.4	1174.73	587.97	392.39
L11	$C_{57}H_{87}N_{15}O_{14}$	1206.4	1206.75	604.02	403.01
L12	$C_{63}H_{101}N_{17}O_{12}$	1288.6	1288.92	645.06	430.47
L13	$C_{66}H_{97}N_{17}O_{10}$	1288.6	1288.82	645.08	430.47
L14	$C_{73}H_{97}N_{17}O_{12}$	1404.7	1405.0	703.09	469.08
L15	$C_{77}H_{99}N_{19}O_{10}$	1450.8	1451.06	726.06	484.42
L16	$C_{61}H_{89}N_{17}O_{10}$	1220.5	1220.87	611.03	407.74
L17	$C_{61}H_{89}N_{17}O_{12}$	1252.5	1252.85	627.03	418.46
L18	$C_{67}H_{103}N_{19}O_{10}$	1334.7	1334.78	668.15	445.80
L19	$C_{50}H_{87}N_{15}O_{10}$	1058.3	1058.84	530.03	353.69
L20	$C_{57}H_{87}N_{15}O_{12}$	1174.4	1174.71	588.11	392.41
L21	$C_{61}H_{89}N_{17}O_{10}$	1220.5	1220.91	611.16	407.78
L22	$C_{45}H_{79}N_{15}O_{10}$	990.2	–	495.7	–
L23	$C_{45}H_{79}N_{15}O_{12}$	1022.2	–	511.94	–
L24	$C_{51}H_{93}N_{17}O_{10}$	1104.4	–	553.12	–

0.1% CF_3COOH over 20 min). CD Spectra were measured in H_2O at pH 5.0 and 20°, or for **L15** in MeOH/H_2O 1:1, at a peptide concentration of *ca.* 150–300 μM. The peptides were analyzed by ES-MS (*Table 4*).

NMR and Structure Calculations. The 1D and 2D NMR spectra of **1** and **2** were recorded at 290 and 300 K, resp., at 600 MHz (*Bruker-AMX600* spectrometer), typically at a peptide concentration of ca. 20 mg/ml in H_2O/D_2O 9:1 (pH 5). The mimetics **L2** – **L24** were measured under the same conditions at 300 K. The H_2O signal was presaturated. *Felix* software (*MSI*, San Diego) was used for the analysis of 2D spectra. Assignments of ^1H spectra were made by standard methods [22] using 2D TOCSY, DQF-COSY, and NOESY and/or ROESY.

For the structure calculations of **1** and **2**, NOEs were determined from NOESY spectra measured with mixing times of 40, 80, 120, and 250 ms, with 2048 × 256 data points zero-filled prior to *Fourier* transformation to 4096 × 2048, and transformed with a sine-bell weighting function. Cross-peak volumes were determined by integration, and the build-up curves were checked to ensure a smooth exponential increase in peak intensity for all NOEs used in deriving distance restraints. To derive NOE distance restraints, it was assumed that the initial rate approximation is valid, and that each peptide rotates as a single isotropic rotor. The relative cross-peak volumes were assumed to be proportional to r^{-6}, and were used to derive distance restraints for simulated-annealing (SA) calculations, performed using methods described in detail elsewhere [23].

For MD simulations with and without TA-DR, the GROMOS96 suite of programs [25] was used with the 43A1 force field, at 300 K and 1 atm pressure, and with periodic boundary conditions. Arg, Glu, and Lys residues were simulated with charged side chains and Na^+ or Cl^- counterions for electrical neutrality. The upper distance restraints were the exact values obtained from NOE build-up curves, where necessary with pseudoatom corrections, a memory decay time $\tau_{dr} = 50$ ps, and a force constant $K_{dr} = 1000$ kJ mol^{-1} nm^{-2}. The starting structure was one of the lowest-energy SA structures embedded in a truncated octahedral box filled with SPC H_2O molecules. The temp. was held constant by weak coupling ($\tau_T = 0.1$ ps) to an external bath at 300 K. The SHAKE algorithm was used to maintain bond lengths with a relative precision of 10^{-4}, and the integrator time step was 0.002 ps. Nonbonded interactions evaluated at every step were within a short-range cut-off of 8 Å. For

long-range interactions, calculated every 5 steps, the cut-off was 14 Å. Structures were saved for analysis every 100 steps (0.2 ps). After short simulations to relax the solute and solvent, the simulations with and without TA-DR were each run for 2 ns.

REFERENCES

[1] D. P. Fairlie, M. L. West, A. K. Wong, *Curr. Med. Chem.* **1998**, *5*, 29.
[2] D. Obrecht, M. Altorfer, J. A. Robinson, *Adv. Med. Chem.* **1999**, *4*, 1.
[3] 'Peptide Secondary Structure Mimetics', Ed. M. Kahn, Tetrahedron Symposia in Print, 1993, 50, 3433.
[4] M. Feigel, *J. Am. Chem. Soc.* **1986**, *108*, 181.
[5] K. Müller, D. Obrecht, A. Knierzinger, C. Stankovic, C. Spiegler, W. Bannwarth, A. Trzeciak, G. Englert, A. M. Labhardt, P. Schönholzer, in 'Perspectives in Medicinal Chemistry', Eds. B. Testa, E. Kyburz, W. Fuhrer and R. Giger, Verlag Helvetica Chimica Acta, Basel, 1993; p. 513.
[6] C. L. Nesloney, J. W. Kelly, *J. Am. Chem. Soc.* **1996**, *118*, 5836.
[7] C. L. Nesloney, J. W. Kelly, *J. Org. Chem.* **1996**, *61*, 3127.
[8] S. H. Gellman, *Curr. Opin. Chem. Biol.* **1998**, *2*, 717.
[9] J. S. Nowick, *Acc. Chem. Res.* **1999**, *32*, 287.
[10] D. S. Kemp, Z. Q. Li, *Tetrahedron Lett.* **1995**, *36*, 4179.
[11] D. S. Kemp, B. R. Bowen, C. C. Muendel, *J. Org. Chem.* **1990**, *55*, 4650.
[12] S. R. Raghothama, S. K. Awasthi, P. Balaram, *J. Chem. Soc.*, *Perkin Trans.* 2 **1998**, 137.
[13] R. R. Gardner, G.-B. Liang, S. H. Gellman, *J. Am. Chem. Soc.* **1999**, *121*, 1806.
[14] M. Favre, K. Moehle, L. Jiang, B. Pfeiffer, J. A. Robinson, *J. Am. Chem. Soc.* **1999**, *121*, 2679.
[15] J. Späth, F. Stuart, L. Jiang, J. A. Robinson, *Helv. Chim. Acta* **1998**, *81*, 1726.
[16] M. E. Pfeifer, J. A. Robinson, *Chem. Commun.* **1998**, 1977.
[17] J. W. Bean, K. D. Kopple, C. E. Peishoff, *J. Am. Chem. Soc.* **1992**, *114*, 5328.
[18] Y. Takeuchi, G. R. Marshall, *J. Am. Chem. Soc.* **1998**, *120*, 5363.
[19] D. K. Chalmers, G. R. Marshall, *J. Am. Chem. Soc.* **1995**, *117*, 5927.
[20] C. Oefner, A. D'Arcy, F. K. Winkler, B. Eggimann, M. Hosang, *EMBO J.* **1992**, *11*, 3921.
[21] E. Atherton, R. C. Sheppard, 'Solid Phase Peptide Synthesis – A Practical Approach', IRL Press, Oxford, 1989.
[22] K. Wüthrich, 'NMR of Proteins and Nucleic Acids', Wiley-Interscience, New York, 1986.
[23] C. Bisang, C. Weber, J. A. Robinson, *Helv. Chim. Acta* **1996**, *79*, 1825.
[24] C. Bisang, L. Jiang, E. Freund, F. Emery, C. Bauch, H. Matile, G. Pluschke, J. A. Robinson, *J. Am. Chem. Soc.* **1998**, *120*, 7439.
[25] W. F. van Gunsteren, S. R. Billeter, A. A. Eising, P. H. Hünenberger, P. Krüger, A. E. Mark, W. R. P. Scott, I. G. Tironi, 'Biomolecular Simulation: The GROMOS96 Manual and User Guide', Hochschulverlag AG an der ETH Zürich, Zürich, 1996.
[26] B. L. Sibanda, T. L. Blundell, J. M. Thornton, *J. Mol. Biol.* **1989**, *206*, 759.
[27] B. L. Sibanda, J. M. Thornton, *J. Mol. Biol.* **1993**, *229*, 428.
[28] D. Schilling, J. D. Reid, A. Hujer, D. Morgan, E. Demoll, P. Bummer, R. A. Fenstermaker, D. M. Kaetzel, *Biochem. J.* **1998**, *333*, 637.
[29] J. Kreysing, A. Östman, M. van de Poll, G. Bäckström, C.-H. Heldin, *FEBS Lett.* **1996**, *385*, 181.
[30] R. A. Fenstermaker, E. Poptic, T. L. Bonfield, T. C. Knauss, L. Corsillo, J. F. Piskurich, C. S. Kaetzel, J. E. Jentoft, C. Gelfand, P. E. DiCorleto, D. M. Kaetzel, *J. Biol. Chem.* **1993**, *268*, 10482.
[31] A. A. Bogan, K. S. Thorn, *J. Mol. Biol.* **1998**, 280, 1.
[32] H. Brückner, C. Keller-Hoehl, *Chromatographia* **1990**, *30*, 621.
[33] 'Circular Dichroism and the Conformational Analysis of Biomolecules', Ed. G. D. Fasman, Plenum Press, New York and London, 1996.

Received April 19, 2000